

Non-Hermitian Skin Effect and Chiral Damping in Open Quantum Systems

Fei Song, Shunyu Yao, and Zhong Wang^{✉*}

Institute for Advanced Study, Tsinghua University, Beijing 100084, China



(Received 24 April 2019; published 21 October 2019; corrected 24 October 2019)

One of the unique features of non-Hermitian Hamiltonians is the non-Hermitian skin effect, namely, that the eigenstates are exponentially localized at the boundary of the system. For open quantum systems, a short-time evolution can often be well described by the effective non-Hermitian Hamiltonians, while long-time dynamics calls for the Lindblad master equations, in which the Liouvillian superoperators generate time evolution. In this Letter, we find that Liouvillian superoperators can exhibit the non-Hermitian skin effect, and uncover its unexpected physical consequences. It is shown that the non-Hermitian skin effect dramatically shapes the long-time dynamics, such that the damping in a class of open quantum systems is algebraic under periodic boundary conditions but exponential under open boundary conditions. Moreover, the non-Hermitian skin effect and non-Bloch bands cause a chiral damping with a sharp wave front. These phenomena are beyond the effective non-Hermitian Hamiltonians; instead, they belong to the non-Hermitian physics of full-fledged open quantum dynamics.

DOI: 10.1103/PhysRevLett.123.170401

Non-Hermitian Hamiltonians provide a natural framework for a wide range of phenomena such as photonic systems with loss and gain [1–5], open quantum systems [6–16], and quasiparticles with finite lifetimes [17–21]. Recently, the interplay of non-Hermiticity and topological phases have been attracting growing attention. Considerable attention has been focused on non-Hermitian bulk-boundary correspondence [22–34], new topological invariants [24,25,27,31,35–42], generalizations of topological insulators [25,43–56] and semimetals [57–67], and novel topological classifications [68–70], among other interesting theoretical [71–81] and experimental [82–87] investigations.

One of the remarkable phenomena of non-Hermitian systems is the non-Hermitian skin effect [24,26] (NHSE), namely, that the majority of eigenstates of a non-Hermitian operator are localized at boundaries, which suggests the non-Bloch bulk-boundary correspondence [24,28] and non-Bloch band theory based on the generalized Brillouin zone [24,25,31,37,40]. Broader implications of NHSE have been under investigation [25,32,33,37,58,88–99]. Very recently, NHSE has been observed in experiments [100–102].

In open quantum systems, non-Hermiticity naturally arises in the Lindblad master equation that governs the time evolution of density matrix (see, e.g., Refs. [8,9]):

$$\frac{d\rho}{dt} = -i[H, \rho] + \sum_{\mu} (2L_{\mu}\rho L_{\mu}^{\dagger} - \{L_{\mu}^{\dagger}L_{\mu}, \rho\}) \equiv \mathcal{L}\rho, \quad (1)$$

where H is the Hamiltonian, L_{μ} 's are the Lindblad dissipators describing quantum jumps due to coupling to the environment, and \mathcal{L} is called the Liouvillian superoperator. Before the occurrence of a jump, the short-time

evolution follows the effective non-Hermitian Hamiltonian $H_{\text{eff}} = H - i \sum_{\mu} L_{\mu}^{\dagger} L_{\mu}$ as $d\rho/dt = -i(H_{\text{eff}}\rho - \rho H_{\text{eff}}^{\dagger})$ [11,12,103].

It is generally believed that when the system size is not too small, the effect of the boundary condition is insignificant. As such, the periodic boundary condition is commonly adopted, though the open-boundary condition is more relevant to experiments. In this Letter, we show that the long-time Lindblad dynamics of an open-boundary system dramatically differ from that of a periodic-boundary system. Furthermore, this is related to the NHSE of the damping matrix derived from the Liouvillian. Notable examples are found that the long-time damping is algebraic (i.e., power law) under periodic boundary conditions while exponential under open boundary conditions. Moreover, NHSE implies that the damping is unidirectional, which is dubbed the “chiral damping.” Crucially, the theory is based on the full Liouvillian. Although H_{eff} may be expected to play an important role, it is in fact inessential here (e.g., its having NHSE or not does not matter).

Model.—The system is illustrated in Fig. 1(a). Our Hamiltonian $H = \sum_{ij} h_{ij} c_i^{\dagger} c_j$, where c_i^{\dagger}, c_i are fermion creation and annihilation operators at site i (including additional degrees of freedom such as spin is straightforward). We will consider single particle loss and gain, with loss dissipators $L_{\mu}^l = \sum_i D_{\mu i}^l c_i$ and gain dissipators $L_{\mu}^g = \sum_i D_{\mu i}^g c_i^{\dagger}$, respectively. For concreteness, we take h to be Su-Schrieffer-Heeger (SSH), namely, $h_{ij} = t_1$ and t_2 on adjacent links. A site is also labeled as $i = xs$, where x refers to the unit cell, and $s = A, B$ refers to the sublattice. For simplicity, let each unit cell contain a single loss and gain dissipator (namely, μ is just x):

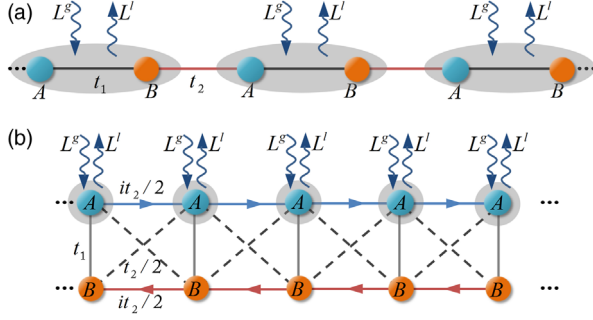


FIG. 1. (a) SSH model with staggered hopping t_1 and t_2 , with the ovals indicating the unit cells. The Bloch Hamiltonian is $h(k) = (t_1 + t_2 \cos k)\sigma_x + t_2 \sin k\sigma_y$. The fermion loss and gain are described by the dissipators L^l and L^g [Eq. (2)] in the master equation framework. (b) A different realization of the same model. The hopping Hamiltonian $h(k) = (t_1 + t_2 \cos k)\sigma_x + t_2 \sin k\sigma_z$, and the dissipators are $L_x^l = \sqrt{\gamma_l}c_{xA}$ and $L_x^g = \sqrt{\gamma_g}c_{xA}^\dagger$, (b) is equivalent to (a) via a basis change $\sigma_y \leftrightarrow \sigma_z$. Because gain and loss is on site, (b) is more feasible experimentally.

$$\begin{aligned} L_x^l &= \sqrt{\gamma_l/2}(c_{xA} - ic_{xB}), \\ L_x^g &= \sqrt{\gamma_g/2}(c_{xA}^\dagger + ic_{xB}^\dagger); \end{aligned} \quad (2)$$

in other words, $D_{x,xA}^l = iD_{x,xB}^l = \sqrt{\gamma_l/2}$, $D_{x,xA}^g = -iD_{x,xB}^g = \sqrt{\gamma_g/2}$. We recognized in Eq. (2) that the $\sigma_y = +1$ states are lost to or gained from the bath. A seemingly different but essentially equivalent realization of the same model is shown in Fig. 1(b), which can be obtained from the initial model [Fig. 1(a)] after a basis change $\sigma_y \leftrightarrow \sigma_z$. Accordingly, the dissipators in Fig. 1(b) are $\sigma_z = 1$ states. As the gain and loss are on site, its experimental implementation is easier. Keeping in mind that Fig. 1(b) shares the same physics, hereafter we focus on the setup in Fig. 1(a).

To see the evolution of the density matrix, it is convenient to monitor the single-particle correlation $\Delta_{ij}(t) = \text{Tr}[c_i^\dagger c_j \rho(t)]$, whose time evolution is $d\Delta_{ij}/dt = \text{Tr}[c_i^\dagger c_j d\rho/dt]$. It follows from Eq. (1) that (see the Supplemental Material [104])

$$\frac{d\Delta(t)}{dt} = i[h^T, \Delta(t)] - \{M_l^T + M_g, \Delta(t)\} + 2M_g, \quad (3)$$

where $(M_g)_{ij} = \sum_\mu D_{\mu i}^{g*} D_{\mu j}^g$ and $(M_l)_{ij} = \sum_\mu D_{\mu i}^{l*} D_{\mu j}^l$, and both M_l and M_g are Hermitian matrices. Majorana versions of Eq. (3) appeared in Refs. [8,16,105]. We can define the damping matrix

$$X = ih^T - (M_l^T + M_g), \quad (4)$$

which recasts Eq. (3) as

$$\frac{d\Delta(t)}{dt} = X\Delta(t) + \Delta(t)X^\dagger + 2M_g. \quad (5)$$

The steady state correlation $\Delta_s = \Delta(\infty)$, to which long-time evolution of any initial state converges, is determined by $d\Delta_s/dt = 0$, or $X\Delta_s + \Delta_s X^\dagger + 2M_g = 0$. In this Letter, we are concerned mainly about the dynamics, especially the speed of converging to the steady state; therefore, we shall focus on the deviation $\tilde{\Delta}(t) = \Delta(t) - \Delta_s$, whose evolution is $d\tilde{\Delta}(t)/dt = X\tilde{\Delta}(t) + \tilde{\Delta}(t)X^\dagger$, which is readily integrated to

$$\tilde{\Delta}(t) = e^{Xt}\tilde{\Delta}(0)e^{X^\dagger t}. \quad (6)$$

We can write X in terms of right and left eigenvectors [106],

$$X = \sum_n \lambda_n |u_{Rn}\rangle \langle u_{Ln}|, \quad (7)$$

and express Eq. (6) as

$$\tilde{\Delta}(t) = \sum_{n,n'} \exp[(\lambda_n + \lambda_{n'}^*)t] |u_{Rn}\rangle \langle u_{Ln}| \tilde{\Delta}(0) |u_{Ln'}\rangle \langle u_{Rn'}|. \quad (8)$$

By the dissipative nature, $\text{Re}(\lambda_n) \leq 0$ always holds true. The Liouvillian gap $\Lambda = \min[2\text{Re}(-\lambda_n)]$ is crucial for the long-time dynamics. A finite gap implies exponential convergence towards the steady state, while a vanishing gap implies algebraic convergence [107].

Periodic chain.—Let us study the periodic boundary chain, for which the momentum space is more convenient. It can be readily found that $h(k) = (t_1 + t_2 \cos k)\sigma_x + t_2 \sin k\sigma_y$ and

$$M_l(k) = \frac{\gamma_l}{2}(1 + \sigma_y), M_g(k) = \frac{\gamma_g}{2}(1 - \sigma_y). \quad (9)$$

These $M(k)$ matrices are k independent because the gain and loss dissipators are intracell. The Fourier transformation of X is $X(k) = ih^T(-k) - M_l^T(-k) - M_g(k)$ (the minus sign in $-k$ comes from matrix transposition); therefore, the damping matrix in momentum space reads

$$X(k) = i \left[(t_1 + t_2 \cos k)\sigma_x + \left(t_2 \sin k - i\frac{\gamma}{2} \right) \sigma_y \right] - \frac{\gamma}{2} I, \quad (10)$$

where $\gamma \equiv \gamma_l + \gamma_g$. If we take the realization in Fig. 1(b) instead of Fig. 1(a), the only modification to $X(k)$ is a basis change $\sigma_y \rightarrow \sigma_z$ in Eq. (10), with the physics unchanged. Diagonalizing $X(k)$, we find that the Liouvillian gap $\Lambda = 0$ for $t_1 \leq t_2$, while the gap opens for $t_1 > t_2$ [Fig. 2(b)]. The damping rate is therefore expected to be algebraic and exponential in each case, respectively. To confirm this, we numerically calculate the site-averaged fermion number

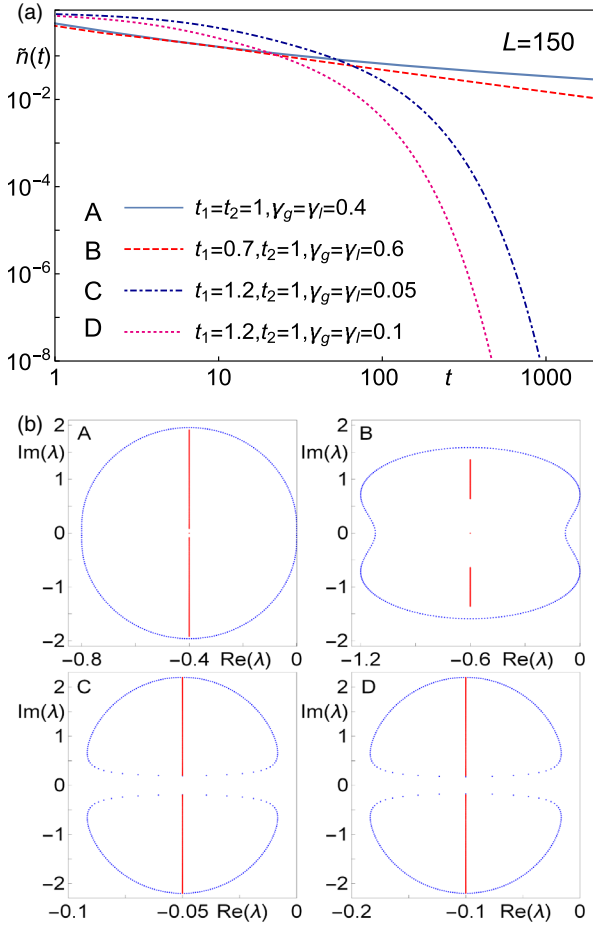


FIG. 2. (a) The damping of the fermion number towards the steady state of a periodic boundary chain with length $L = 150$ (unit cell). The damping is algebraic for cases A, B with $t_1 \leq t_2$, while exponential for C, D with $t_1 > t_2$. The initial state is the completely filled state $\prod_{x,s} c_{xs}^\dagger |0\rangle$. (b) The eigenvalues of the damping matrix X . Blue: periodic boundary; Red: open boundary. The Liouvillian gap of the periodic-boundary chain vanishes for A and B, while it is nonzero for C and D. For the open-boundary chain, the Liouvillian gap is nonzero in all four cases. This drastic spectral distinction between open and periodic boundary comes from the NHSE (see text).

deviation from the steady state, defined as $\tilde{n}(t) = \sqrt{\sum_x \tilde{n}_x^2(t)}/L$, where $\tilde{n}_x(t) = n_x(t) - n_x(\infty)$ with $n_x(t) = n_{xA}(t) + n_{xB}(t)$, $n_{xs} \equiv \Delta_{xs,xs}$ being the fermion number at site xs . The results are consistent with the vanishing (nonzero) gap in the $t_1 \leq t_2$ ($t_1 > t_2$) case [Fig. 2(a)].

Although our focus here is the damping dynamics, we also give the steady state. In fact, our M_l and M_g satisfy $M_l^T + M_g = M_g \gamma / \gamma_g$, which guarantees that $\Delta_s = (\gamma_g / \gamma) I_{2L \times 2L}$ is the steady state solution. It is independent of boundary conditions.

Now we show the direct relation between the algebraic damping and the vanishing gap of X . The eigenvalues of $X(k)$ are

$$\lambda_{\pm}(k) = -\gamma/2 \pm i\sqrt{(t_1^2 + t_2^2 + 2t_1 t_2 \cos k - \gamma^2/4) - it_2 \gamma \sin k}. \quad (11)$$

Let us consider $t_1 = t_2 \equiv t_0$ for concreteness (case A in Fig. 2), then $\lambda_-(\pi) = 0$ and the expansion in $\delta k \equiv k - \pi$ reads

$$\lambda_-(\pi + \delta k) \approx -it_0 \delta k - \frac{t_0^2}{4\gamma} (\delta k)^4. \quad (12)$$

Now Eq. (7) becomes $X = \sum_{k,\alpha=\pm} \lambda_{\alpha}(k) |u_{Rk\alpha}\rangle \langle u_{Lk\alpha}|$, and Eq. (8) reads

$$\tilde{\Delta}(t) = \sum_{kk',\alpha\alpha'} e^{\lambda_{\alpha}(k)t + \lambda_{\alpha'}^*(k')t} |u_{Rk\alpha}\rangle \langle u_{Lk\alpha}| \tilde{\Delta}(0) |u_{Lk'\alpha'}\rangle \langle u_{Rk'\alpha'}|. \quad (13)$$

For the initial state with translational symmetry, we have $\langle u_{Lk\alpha} | \tilde{\Delta}(0) | u_{Lk'\alpha'} \rangle = \delta_{kk'} \langle u_{Lk\alpha} | \tilde{\Delta}(0) | u_{Lk\alpha} \rangle$. The long-time behavior of $\tilde{\Delta}(t)$ is dominated by the $\alpha = \alpha' = -$ sector, which provides a decay factor $\sum_{\delta k} \exp(2\text{Re}[\lambda_-(\pi + \delta k)]t) \approx \int d(\delta k) \exp[-(t_0^2/2\gamma)(\delta k)^4 t] \sim t^{-1/4}$. Similarly, for $t_1 < t_2$ we have $\tilde{\Delta}(t) \sim t^{-1/2}$.

Chiral damping.—Now we turn to the open boundary chain. Although the physical interpretation is quite different, our X matrix resembles the non-Hermitian SSH Hamiltonian [24,39], as can be appreciated from Eq. (10). Remarkably, all the eigenstates of X are exponentially localized at the boundary (i.e., NHSE [24]). As such, the eigenvalues of open boundary X cannot be obtained from $X(k)$ with real-valued k ; instead, we have to take complex-valued wave vectors $k + i\kappa$. In other words, the usual Bloch phase factor e^{ik} living in the unit circle is replaced by $\exp[i(k + i\kappa)]$ inhabiting a generalized Brillouin zone [24], whose shape can be precisely calculated in the non-Bloch band theory [24,25,31,37,40].

From the non-Bloch band theory [24], we find that $\kappa = -\ln \sqrt{|(t_1 + \gamma/2)/(t_1 - \gamma/2)|}$, and that the eigenvalues of X of an open boundary chain are $\lambda_{\pm}(k + i\kappa)$, where λ_{\pm} are the $X(k)$ eigenvalues given in Eq. (11). We can readily check that, for $|\gamma| < 2|t_1|$,

$$\lambda_{\pm}(k + i\kappa) = -\frac{\gamma}{2} \pm iE(k), \quad (14)$$

where $E(k) = \sqrt{t_1^2 + t_2^2 - (\gamma^2/4) + 2t_2 \sqrt{t_1^2 - (\gamma^2/4)} \cos k}$, which is real. We have also numerically diagonalized X for a long open chain [red dots in Fig. 2(b)], which confirms Eq. (14). An immediate feature of Eq. (14) is that the real part is a constant, $-\gamma/2$, which is consistent with the numerical spectrums [Fig. 2(b)]. We note that the analytic results based on the generalized Brillouin zone produce the continuum bands only, and the isolated topological edge

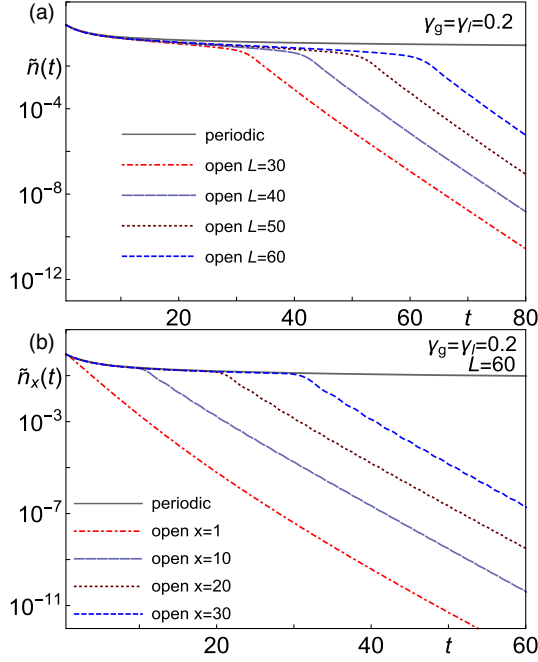


FIG. 3. (a) The particle number damping of a periodic boundary chain (solid curve) and open-boundary chains for several chain length L . The long-time damping of a periodic chain follows a power law, while the open boundary chain follows an exponential law after an initial power law stage. (b) The site-resolved damping. The left end ($x = 1$) enters the exponential stage from the very beginning, followed sequentially by other sites. For both (a) and (b), the initial state is the completely filled state $\prod_{x,s} c_{xs}^\dagger |0\rangle$, therefore, $\Delta(0)$ the identity matrix $I_{2L \times 2L}$. $t_1 = t_2 = 1$, $\gamma_g = \gamma_l = 0.2$.

modes [Fig. 2(b), *A* and *B* panels] are not contained in Eq. (14), though they can be inferred from the non-Bloch bulk-boundary correspondence [24,28]. Here, we focus on bulk dynamics, and these topological edge modes do not play important roles [108].

It follows from Eq. (14) that the Liouvillian gap $\Lambda = \gamma$; therefore, we expect an exponential long-time damping of $\tilde{\Delta}(t)$. This behavior is confirmed by numerical simulation [Fig. 3(a)]. Before entering the exponential stage, there is an initial period of algebraic damping whose duration grows with chain length L [Fig. 3(a)]. To better understand this feature, we plot the damping in each unit cell [Fig. 3(b)]. We find that the left end ($x = 1$) enters the exponential damping immediately, and other sites enter the exponential stage sequentially, according to their distances to the left end. As such, there is a “damping wave front” traveling from the left to right. This is dubbed a chiral damping, which can be intuitively related to the fact that all eigenstates of X are localized at the right end [24].

More intuitively, the damping of $\tilde{n}_x(t) = n_x(t) - n_x(\infty)$ is shown in Fig. 4(a). In the periodic boundary chain it follows a slow power law. In the open boundary chain, a right-moving wave front is seen. After the wave front

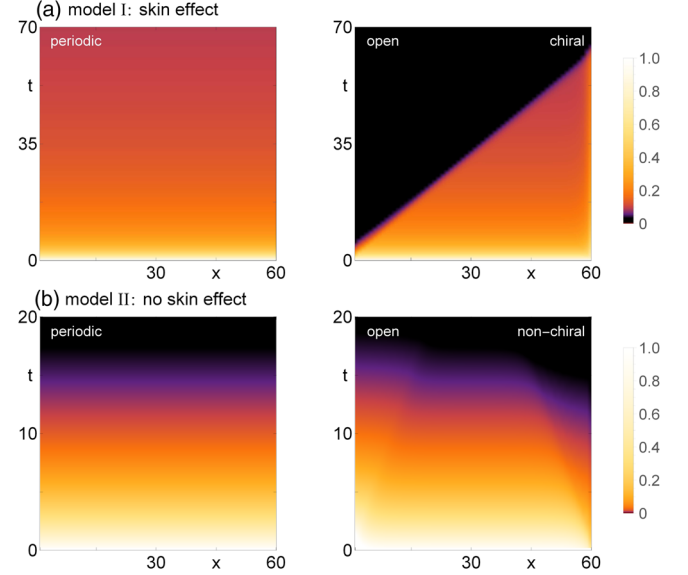


FIG. 4. Time evolution of $\tilde{n}_x(t) = n_x(t) - n_x(\infty)$, which shows damping of particle number $n_x(t)$ towards the steady state. (a) $\tilde{n}_x(t)$ of the main model with dissipators given by Eq. (2) (referred to as model I). Left: periodic boundary; Right: open boundary. The chiral damping is clearly seen in the open boundary case. The dark region corresponds to the exponential damping stage seen in Fig. 3. (b) $\tilde{n}_x(t)$ of model II, whose damping matrix X [Eq. (15)] has no NHSE. The Liouvillian gap is nonzero and the same for periodic and open boundary chains. Common parameters: $t_1 = t_2 = 1$; $\gamma_g = \gamma_l = 0.2$.

passes by x , the algebraically decaying $\tilde{n}_x(t)$ enters the exponential decay stage and rapidly diminishes.

The wave front can be understood as follows. According to Eq. (6), the damping of $\tilde{\Delta}(t)$ is determined by the evolution under $\exp(Xt)$, which is just the evolution under $\exp(-\gamma t/2) \exp(-iH_{\text{SSH}}t)$, where H_{SSH} is the non-Hermitian SSH Hamiltonian [24] (with an unimportant sign difference). Now the propagator $\langle x_s | \exp(-iH_{\text{SSH}}t) | x' s' \rangle$ can be decomposed as propagation of various momentum modes with velocity $v_k = \partial E / \partial k$. Because of the presence of an imaginary part κ in the momentum, propagation from x' to x acquires an $\exp[-\kappa(x - x')]$ factor. If this factor can compensate $\exp(-\gamma t/2)$, exponential damping can be evaded, giving way to a power law damping. For simplicity we take γ small, so that $\kappa \approx -\gamma/2t_1$; therefore, $\exp[-\kappa(x - x')] \approx \exp[v_k(\gamma/2t_1)t]$ and the damping of propagation from x' to x is $\exp[(-\gamma/2 + v_k\gamma/2t_1)t]$ for the k mode. By a straightforward calculation, we have $\max(v_k) = t_2$ (for $t_1 > t_2$) or $\sqrt{t_1^2 - \gamma^2/4} \approx t_1$ (for $t_1 \leq t_2$). Let us consider $t_1 \leq t_2$ first. When $x > \max(v_k)t$, the propagation from $x' = x - \max(v_k)t$ to x carries a factor $\exp\{-\gamma/2 + \max(v_k)\gamma/2t_1\}t = 1$; while for $x < \max(v_k)t$, we need the nonexistent $x' = x - \max(v_k)t < 0$; therefore, compensation is impossible and we have exponential damping. This indicates a wave front at $x = \max(v_k)t$. For

$t_1 = t_2 = 1$, we have $\max(v_k) \approx 1$, which is consistent with the wave front velocity (≈ 1) in Fig. 4(a).

As a comparison, we introduce the model II (the model studied so far is referred to as “model I”) that differs from model I only in L_x^g , which is now $L_x^g = \sqrt{(\gamma_g/2)}(c_{xA}^\dagger - ic_{xB}^\dagger)$ [compare it with Eq. (2)]. The damping matrix is

$$X(k) = i \left[(t_1 + t_2 \cos k) \sigma_x + \left(t_2 \sin k - i \frac{\gamma_l - \gamma_g}{2} \right) \sigma_y \right] - \frac{\gamma}{2} I, \quad (15)$$

which has no NHSE when $\gamma_l = \gamma_g$. Accordingly, the open and periodic boundary chains have the same Liouvillian gap, and chiral damping is absent [Fig. 4(b)].

In realistic systems, there may be disorders, fluctuations of parameters, and other imperfections. Fortunately, the main results here are based on the presence of NHSE, which is a quite robust phenomenon unchanged by modest imperfections. As such, it is expected that our predictions are robust and observable.

Final remarks.—(i) The chiral damping originates from the NHSE of the damping matrix X rather than the effective non-Hermitian Hamiltonian. Unlike the damping matrix, the effective non-Hermitian Hamiltonian describes short time evolution. It is found to be $H_{\text{eff}} = \sum_{ij} c_i^\dagger (h_{\text{eff}})_{ij} c_j - i\gamma_g L$, where h_{eff} , written in momentum space, is $h_{\text{eff}}(k) = (t_1 + t_2 \cos k) \sigma_x + \{t_2 \sin k - i[(\gamma_l - \gamma_g)/2]\} \sigma_y - i\{[(\gamma_l - \gamma_g)/2]\} I$. For $\gamma_g = \gamma_l$, h_{eff} has no NHSE, though X has. Although damping matrices with NHSE can arise quite naturally (e.g., in Fig. 1), none of the previous models (e.g., Ref. [111]) we have checked has NHSE.

(ii) The periodic-open contrast between the slow algebraic and fast exponential damping has important implications for experimental preparation of steady states (e.g., in cold atom systems). In the presence of NHSE, approaching the steady states in open-boundary systems can be much faster than estimations based on periodic boundary condition.

(iii) It is interesting to investigate other rich aspects of non-Hermitian physics such as PT symmetry breaking [112] in this platform (Here, we have focused on the cases that the open-boundary iX is essentially PT symmetric, meaning that the real parts of X eigenvalues are constant).

(iv) When fermion-fermion interactions are included, higher-order correlation functions are coupled to the two-point ones, and approximations (such as truncations) are called for. Moreover, the steady states can be multiple [113,114], in which case the damping matrix depends on the steady state approached, leading to even richer chiral damping behaviors. These possibilities will be left for future studies.

This work is supported by NSFC (Grant No. 11674189).

*wangzhongemail@gmail.com

- [1] L. Feng, R. El-Ganainy, and L. Ge, Non-hermitian photonics based on parity–time symmetry, *Nat. Photonics* **11**, 752 (2017).
- [2] R. El-Ganainy, K. G. Makris, M. Khajavikhan, Z. H. Musslimani, S. Rotter, and D. N. Christodoulides, Non-hermitian physics and pt symmetry, *Nat. Phys.* **14**, 11 (2018).
- [3] T. Ozawa, H. M. Price, A. Amo, N. Goldman, M. Hafezi, L. Lu, M. C. Rechtsman, D. Schuster, J. Simon, O. Zilberberg, and I. Carusotto, Topological photonics, *Rev. Mod. Phys.* **91**, 015006 (2019).
- [4] B. Peng, Ş. K. Özdemir, S. Rotter, H. Yilmaz, M. Liertzer, F. Monifi, C. M. Bender, F. Nori, and L. Yang, Loss-induced suppression and revival of lasing, *Science* **346**, 328 (2014).
- [5] L. Feng, Y.-L. Xu, W. S. Fegadolli, M.-H. Lu, J. E. B. Oliveira, V. R. Almeida, Y.-F. Chen, and A. Scherer, Experimental demonstration of a unidirectional reflectionless parity-time metamaterial at optical frequencies, *Nat. Mater.* **12**, 108 (2013).
- [6] I. Rotter, A non-Hermitian Hamilton operator and the physics of open quantum systems, *J. Phys. A* **42**, 153001 (2009).
- [7] B. Zhen, C. W. Hsu, Y. Igarashi, L. Lu, I. Kaminer, A. Pick, S.-L. Chua, J. D. Joannopoulos, and M. Soljačić, Spawning rings of exceptional points out of dirac cones, *Nature (London)* **525**, 354 (2015).
- [8] S. Diehl, E. Rico, M. A. Baranov, and P. Zoller, Topology by dissipation in atomic quantum wires, *Nat. Phys.* **7**, 971 (2011).
- [9] F. Verstraete, M. M. Wolf, and J. I. Cirac, Quantum computation and quantum-state engineering driven by dissipation, *Nat. Phys.* **5**, 633 (2009).
- [10] S. Malzard, C. Poli, and H. Schomerus, Topologically Protected Defect States in Open Photonic Systems with Non-Hermitian Charge-Conjugation and Parity-Time Symmetry, *Phys. Rev. Lett.* **115**, 200402 (2015).
- [11] J. Dalibard, Y. Castin, and K. Mølmer, Wave-Function Approach to Dissipative Processes in Quantum Optics, *Phys. Rev. Lett.* **68**, 580 (1992).
- [12] H. J. Carmichael, Quantum Trajectory Theory for Cascaded Open Systems, *Phys. Rev. Lett.* **70**, 2273 (1993).
- [13] J. Anglin, Cold, Dilute, Trapped Bosons as an Open Quantum System, *Phys. Rev. Lett.* **79**, 6 (1997).
- [14] Y. Choi, S. Kang, S. Lim, W. Kim, J.-R. Kim, J.-H. Lee, and K. An, Quasieigenstate Coalescence in an Atom-Cavity Quantum Composite, *Phys. Rev. Lett.* **104**, 153601 (2010).
- [15] S. Diehl, A. Micheli, A. Kantian, B. Kraus, H. P. Büchler, and P. Zoller, Quantum states and phases in driven open quantum systems with cold atoms, *Nat. Phys.* **4**, 878 (2008).
- [16] C. E. Bardyn, M. A. Baranov, C. V. Kraus, E. Rico, A. İmamoğlu, P. Zoller, and S. Diehl, Topology by dissipation, *New J. Phys.* **15**, 085001 (2013).
- [17] V. Kozii and L. Fu, Non-hermitian topological theory of finite-lifetime quasiparticles: Prediction of bulk Fermi arc due to exceptional point, [arXiv:1708.05841](https://arxiv.org/abs/1708.05841).

- [18] M. Papaj, H. Isobe, and L. Fu, Nodal arc of disordered Dirac fermions and non-Hermitian band theory, *Phys. Rev. B* **99**, 201107 (2019).
- [19] H. Shen and L. Fu, Quantum Oscillation from in-Gap States and a Non-Hermitian Landau Level Problem, *Phys. Rev. Lett.* **121**, 026403 (2018).
- [20] H. Zhou, C. Peng, Y. Yoon, C. W. Hsu, K. A. Nelson, L. Fu, J. D. Joannopoulos, M. Soljačić, and B. Zhen, Observation of bulk Fermi arc and polarization half charge from paired exceptional points, *Science* **359**, 1009 (2018).
- [21] T. Yoshida, R. Peters, and N. Kawakami, Non-Hermitian perspective of the band structure in heavy-fermion systems, *Phys. Rev. B* **98**, 035141 (2018).
- [22] H. Shen, B. Zhen, and L. Fu, Topological Band Theory for Non-Hermitian Hamiltonians, *Phys. Rev. Lett.* **120**, 146402 (2018).
- [23] T. E. Lee, Anomalous Edge State in a Non-Hermitian Lattice, *Phys. Rev. Lett.* **116**, 133903 (2016).
- [24] S. Yao and Z. Wang, Edge States and Topological Invariants of Non-Hermitian Systems, *Phys. Rev. Lett.* **121**, 086803 (2018).
- [25] S. Yao, F. Song, and Z. Wang, Non-Hermitian Chern Bands, *Phys. Rev. Lett.* **121**, 136802 (2018).
- [26] V. M. Martínez Alvarez, J. E. Barrios Vargas, M. Berdakin, and L. E. F. Foa Torres, Topological states of non-Hermitian systems, *Eur. Phys. J. Spec. Top.* **227**, 1295 (2018).
- [27] D. Leykam, K. Y. Bliokh, C. Huang, Y. D. Chong, and F. Nori, E. Modes, Degeneracies, and Topological Numbers in Non-Hermitian Systems, *Phys. Rev. Lett.* **118**, 040401 (2017).
- [28] F. K. Kunst, E. Edvardsson, J. C. Budich, and E. J. Bergholtz, Biorthogonal Bulk-Boundary Correspondence in Non-Hermitian Systems, *Phys. Rev. Lett.* **121**, 026808 (2018).
- [29] Y. Xiong, Why does bulk boundary correspondence fail in some non-Hermitian topological models, *J. Phys. Commun.* **2**, 035043 (2018).
- [30] V. M. Martínez Alvarez, J. E. Barrios Vargas, and L. E. F. Foa Torres, Non-Hermitian robust edge states in one dimension: Anomalous localization and eigenspace condensation at exceptional points, *Phys. Rev. B* **97**, 121401 (2018).
- [31] K. Yokomizo and S. Murakami, Non-Bloch Band Theory of Non-Hermitian Systems, *Phys. Rev. Lett.* **123**, 066404 (2019).
- [32] L. Jin and Z. Song, Bulk-boundary correspondence in a non-Hermitian system in one dimension with chiral inversion symmetry, *Phys. Rev. B* **99**, 081103 (2019).
- [33] H.-G. Zirnstein, G. Refael, and B. Rosenow, Bulk-boundary correspondence for non-Hermitian Hamiltonians via Green functions, [arXiv:1901.11241](https://arxiv.org/abs/1901.11241).
- [34] L. Herviou, J. H. Bardarson, and N. Regnault, Defining a bulk-edge correspondence for non-Hermitian Hamiltonians via singular-value decomposition, *Phys. Rev. A* **99**, 052118 (2019).
- [35] K. Esaki, M. Sato, K. Hasebe, and M. Kohmoto, Edge states and topological phases in non-Hermitian systems, *Phys. Rev. B* **84**, 205128 (2011).
- [36] Z. Gong, Y. Ashida, K. Kawabata, K. Takasan, S. Higashikawa, and M. Ueda, Topological Phases of Non-Hermitian Systems, *Phys. Rev. X* **8**, 031079 (2018).
- [37] T. Liu, Yu.-R. Zhang, Q. Ai, Z. Gong, K. Kawabata, M. Ueda, and F. Nori, Second-Order Topological Phases in Non-Hermitian Systems, *Phys. Rev. Lett.* **122**, 076801 (2019).
- [38] S. Lieu, Topological phases in the non-Hermitian Su-Schrieffer-Heeger model, *Phys. Rev. B* **97**, 045106 (2018).
- [39] C. Yin, H. Jiang, L. Li, R. Lü, and S. Chen, Geometrical meaning of winding number and its characterization of topological phases in one-dimensional chiral non-Hermitian systems, *Phys. Rev. A* **97**, 052115 (2018).
- [40] T.-S. Deng and W. Yi, Non-bloch topological invariants in a non-Hermitian domain wall system, *Phys. Rev. B* **100**, 035102 (2019).
- [41] A. Ghatak and T. Das, New topological invariants in non-Hermitian systems, *J. Phys. Condens. Matter* **31**, 263001 (2019).
- [42] H. Jiang, C. Yang, and S. Chen, Topological invariants and phase diagrams for one-dimensional two-band non-Hermitian systems without chiral symmetry, *Phys. Rev. A* **98**, 052116 (2018).
- [43] G. Harari, M. A. Bandres, Y. Lumer, M. C. Rechtsman, Y. D. Chong, M. Khajavikhan, D. N. Christodoulides, and M. Segev, Topological insulator laser: Theory, *Science*, **359** eaar4003 (2018).
- [44] C. Yuce, Topological phase in a non-Hermitian PT symmetric system, *Phys. Lett. A* **379**, 1213 (2015).
- [45] B. Zhu, R. Lü, and S. Chen, PT symmetry in the non-Hermitian Su-Schrieffer-Heeger model with complex boundary potentials, *Phys. Rev. A* **89**, 062102 (2014).
- [46] S. Lieu, Topological symmetry classes for non-Hermitian models and connections to the bosonic Bogoliubov-de Gennes equation, *Phys. Rev. B* **98**, 115135 (2018).
- [47] C. Yuce, Majorana edge modes with gain and loss, *Phys. Rev. A* **93**, 062130 (2016).
- [48] H. Menke and M. M. Hirschmann, Topological quantum wires with balanced gain and loss, *Phys. Rev. B* **95**, 174506 (2017).
- [49] C. Wang and X. R. Wang, Non-quantized edge channel conductance and zero conductance fluctuation in non-Hermitian Chern insulators, [arXiv:1901.06982](https://arxiv.org/abs/1901.06982).
- [50] T. M. Philip, M. R. Hirsbrunner, and M. J. Gilbert, Loss of hall conductivity quantization in a non-Hermitian quantum anomalous hall insulator, *Phys. Rev. B* **98**, 155430 (2018).
- [51] Yu. Chen and H. Zhai, Hall conductance of a non-Hermitian Chern insulator, *Phys. Rev. B* **98**, 245130 (2018).
- [52] M. R. Hirsbrunner, T. M. Philip, and M. J. Gilbert, Topology and observables of the non-Hermitian Chern insulator, *Phys. Rev. B* **100**, 081104 (2019).
- [53] M. Klett, H. Cartarius, D. Dast, J. Main, and G. Wunner, Relation between PT -symmetry breaking and topologically nontrivial phases in the Su-Schrieffer-Heeger and Kitaev models, *Phys. Rev. A* **95**, 053626 (2017).
- [54] Q.-B. Zeng, Y.-B. Yang, and Y. Xu, Topological non-Hermitian quasicrystals, [arXiv:1901.08060](https://arxiv.org/abs/1901.08060).
- [55] L. Zhou and J. Gong, Non-Hermitian Floquet topological phases with arbitrarily many real-quasienergy edge states, *Phys. Rev. B* **98**, 205417 (2018).
- [56] K. Kawabata, Y. Ashida, H. Katsura, and M. Ueda, Parity-time-symmetric topological superconductor, *Phys. Rev. B* **98**, 085116 (2018).

- [57] Y. Xu, S.-T. Wang, and L.-M. Duan, Weyl Exceptional Rings in a Three-Dimensional Dissipative Cold Atomic Gas, *Phys. Rev. Lett.* **118**, 045701 (2017).
- [58] H. Wang, J. Ruan, and H. Zhang, Non-Hermitian nodal-line semimetals with an anomalous bulk-boundary correspondence, *Phys. Rev. B* **99**, 075130 (2019).
- [59] A. Cerjan, M. Xiao, L. Yuan, and S. Fan, Effects of non-Hermitian perturbations on Weyl Hamiltonians with arbitrary topological charges, *Phys. Rev. B* **97**, 075128 (2018).
- [60] J. C. Budich, J. Carlström, F. K. Kunst, and E. J. Bergholtz, Symmetry-protected nodal phases in non-Hermitian systems, *Phys. Rev. B* **99**, 041406 (2019).
- [61] Z. Yang and J. Hu, Non-Hermitian Hopf-link exceptional line semimetals, *Phys. Rev. B* **99**, 081102 (2019).
- [62] J. Carlström and E. J. Bergholtz, Exceptional links and twisted fermi ribbons in non-Hermitian systems, *Phys. Rev. A* **98**, 042114 (2018).
- [63] R. Okugawa and T. Yokoyama, Topological exceptional surfaces in non-Hermitian systems with parity-time and parity-particle-hole symmetries, *Phys. Rev. B* **99**, 041202 (2019).
- [64] K. Moors, A. A. Zyuzin, A. Yu. Zyuzin, R. P. Tiwari, and T. L. Schmidt, Disorder-driven exceptional lines and fermi ribbons in tilted nodal-line semimetals, *Phys. Rev. B* **99**, 041116 (2019).
- [65] A. A. Zyuzin and A. Yu. Zyuzin, Flat band in disorder-driven non-Hermitian Weyl semimetals, *Phys. Rev. B* **97**, 041203 (2018).
- [66] T. Yoshida, R. Peters, N. Kawakami, and Y. Hatsugai, Symmetry-protected exceptional rings in two-dimensional correlated systems with chiral symmetry, *Phys. Rev. B* **99**, 121101 (2019).
- [67] H. Zhou, J. Y. Lee, S. Liu, and B. Zhen, Exceptional surfaces in pt -symmetric non-Hermitian photonic systems, *Optica* **6**, 190 (2019).
- [68] K. Kawabata, S. Higashikawa, Z. Gong, Y. Ashida, and M. Ueda, Topological unification of time-reversal and particle-hole symmetries in non-Hermitian physics, *Nat. Commun.* **10**, 297 (2019).
- [69] H. Zhou and J. Y. Lee, Periodic table for topological bands with non-Hermitian symmetries, *Phys. Rev. B* **99**, 235112 (2019).
- [70] K. Kawabata, K. Shiozaki, M. Ueda, and M. Sato, Symmetry and topology in non-Hermitian physics, *arXiv*: 1812.09133.
- [71] M. S. Rudner and L. S. Levitov, Topological Transition in a Non-Hermitian Quantum Walk, *Phys. Rev. Lett.* **102**, 065703 (2009).
- [72] A. McDonald, T. Pereg-Barnea, and A. A. Clerk, Phase-Dependent Chiral Transport and Effective Non-Hermitian Dynamics in a Bosonic Kitaev-Majorana Chain, *Phys. Rev. X* **8**, 041031 (2018).
- [73] W. Hu, H. Wang, P. P. Shum, and Y. D. Chong, Exceptional points in a non-hermitian topological pump, *Phys. Rev. B* **95**, 184306 (2017).
- [74] M. G. Silveirinha, Topological theory of non-Hermitian photonic systems, *Phys. Rev. B* **99**, 125155 (2019).
- [75] K. Kawabata, T. Bessho, and M. Sato, Classification of Exceptional Points and Non-Hermitian Topological Semimetals, *Phys. Rev. Lett.* **123**, 066405 (2019).
- [76] J. A. S. Lourenço, R. L. Eneias, and R. G. Pereira, Kondo effect in a \mathcal{PT} -symmetric non-Hermitian Hamiltonian, *Phys. Rev. B* **98**, 085126 (2018).
- [77] W. B. Rui, Y. X. Zhao, and A. P. Schnyder, Topology and exceptional points of massive dirac models with generic non-Hermitian perturbations, *Phys. Rev. B* **99**, 241110 (2019).
- [78] K. Y. Bliokh and F. Nori, Klein-Gordon Representation of Acoustic Waves and Topological Origin of Surface Acoustic Modes, *Phys. Rev. Lett.* **123**, 054301 (2019).
- [79] X.-W. Luo and C. Zhang, Higher-Order Topological Corner States Induced by Gain and Loss, *Phys. Rev. Lett.* **123**, 073601 (2019).
- [80] Z. Ozcakmakli Turker and C. Yuce, Open and closed boundaries in non-Hermitian topological systems, *Phys. Rev. A* **99**, 022127 (2019).
- [81] N. Hatano and D. R. Nelson, Localization Transitions in Non-Hermitian Quantum Mechanics, *Phys. Rev. Lett.* **77**, 570 (1996).
- [82] J. M. Zeuner, M. C. Rechtsman, Y. Plotnik, Y. Lumer, S. Nolte, M. S. Rudner, M. Segev, and A. Szameit, Observation of a Topological Transition in the Bulk of a Non-Hermitian System, *Phys. Rev. Lett.* **115**, 040402 (2015).
- [83] L. Xiao, X. Zhan, Z. H. Bian, K. K. Wang, X. Zhang, X. P. Wang, J. Li, K. Mochizuki, D. Kim, N. Kawakami, W. Yi, H. Obuse, B. C. Sanders, and P. Xue, Observation of topological edge states in parity-time-symmetric quantum walks, *Nat. Phys.* **13**, 1117 (2017).
- [84] C. Poli, M. Bellec, U. Kuhl, F. Mortessagne, and H. Schomerus, Selective enhancement of topologically induced interface states in a dielectric resonator chain, *Nat. Commun.* **6**, 6710 (2015).
- [85] S. Weimann, M. Kremer, Y. Plotnik, Y. Lumer, S. Nolte, K. G. Makris, M. Segev, M. C. Rechtsman, and A. Szameit, Topologically protected bound states in photonic parity-time-symmetric crystals, *Nat. Mater.* **16**, 433 (2017).
- [86] A. Cerjan, S. Huang, M. Wang, K. P. Chen, Y. Chong, and M. C. Rechtsman, Experimental realization of a Weyl exceptional ring, *Nat. Photonics*, **13**, 623 (2019).
- [87] X. Zhan, L. Xiao, Z. Bian, K. Wang, X. Qiu, B. C. Sanders, W. Yi, and P. Xue, Detecting Topological Invariants in Nonunitary Discrete-Time Quantum Walks, *Phys. Rev. Lett.* **119**, 130501 (2017).
- [88] H. Jiang, L.-J. Lang, C. Yang, S.-L. Zhu, and S. Chen, Interplay of non-hermitian skin effects and anderson localization in nonreciprocal quasiperiodic lattices, *Phys. Rev. B* **100**, 054301 (2019).
- [89] C. H. Lee and R. Thomale, Anatomy of skin modes and topology in non-hermitian systems, *Phys. Rev. B* **99**, 201103 (2019).
- [90] C. H. Lee, L. Li, and J. Gong, Hybrid Higher-Order Skin-Topological Modes in Nonreciprocal Systems, *Phys. Rev. Lett.* **123**, 016805 (2019).
- [91] F. K. Kunst and V. Dwivedi, Non-Hermitian systems and topology: A transfer-matrix perspective, *Phys. Rev. B* **99**, 245116 (2019).
- [92] E. Edvardsson, F. K. Kunst, and E. J. Bergholtz, Non-Hermitian extensions of higher-order topological phases

- and their biorthogonal bulk-boundary correspondence, *Phys. Rev. B* **99**, 081302 (2019).
- [93] D. S. Borgnia, A. Jura Kruchkov, and R.-J. Slager, Non-hermitian boundary modes, [arXiv:1902.07217](https://arxiv.org/abs/1902.07217).
- [94] B. X. Wang and C. Y. Zhao, Topological phonon polaritons in one-dimensional non-Hermitian silicon carbide nanoparticle chains, *Phys. Rev. B* **98**, 165435 (2018).
- [95] M. Ezawa, Non-Hermitian boundary and interface states in nonreciprocal higher-order topological metals and electrical circuits, *Phys. Rev. B* **99**, 121411 (2019).
- [96] M. Ezawa, Non-Hermitian higher-order topological states in nonreciprocal and reciprocal systems with their electric-circuit realization, *Phys. Rev. B* **99**, 201411 (2019).
- [97] M. Ezawa, Braiding of Majorana-like corner states in electric circuits and its non-hermitian generalization, *Phys. Rev. B* **100**, 045407 (2019).
- [98] X. Yang, Y. Cao, and Y. Zhai, Non-Hermitian Weyl semimetals: Non-Hermitian skin effect and non-Bloch bulk-boundary correspondence, [arXiv:1904.02492](https://arxiv.org/abs/1904.02492).
- [99] Z.-Y. Ge, Yu-R. Zhang, T. Liu, S.-W. Li, H. Fan, and F. Nori, Topological band theory for non-Hermitian systems from the Dirac equation, *Phys. Rev. B* **100**, 054105 (2019).
- [100] T. Helbig, T. Hofmann, S. Imhof, M. Abdelghany, T. Kiessling, L. W. Molenkamp, C. H. Lee, A. Szameit, M. Greiter, and R. Thomale, Observation of bulk boundary correspondence breakdown in topoelectrical circuits, [arXiv:1907.11562](https://arxiv.org/abs/1907.11562).
- [101] L. Xiao, T. Deng, K. Wang, G. Zhu, Z. Wang, W. Yi, and P. Xue, Observation of non-Hermitian bulk-boundary correspondence in quantum dynamics, [arXiv:1907.12566](https://arxiv.org/abs/1907.12566).
- [102] A. Ghatak, M. Brandenbourger, J. van Wezel, and C. Coulais, Observation of non-Hermitian topology and its bulk-edge correspondence, [arXiv:1907.11619](https://arxiv.org/abs/1907.11619).
- [103] M. Nakagawa, N. Kawakami, and M. Ueda, Non-Hermitian Kondo Effect in Ultracold Alkaline-Earth Atoms, *Phys. Rev. Lett.* **121**, 203001 (2018).
- [104] See Supplemental Material at <http://link.aps.org/supplemental/10.1103/PhysRevLett.123.170401> for the derivation of Eq. (3).
- [105] T. Ž. Prosen and E. Ilievski, Nonequilibrium Phase Transition in a Periodically Driven xy Spin Chain, *Phys. Rev. Lett.* **107**, 060403 (2011).
- [106] As a non-Hermitian matrix, X can have exceptional points, and we have checked that our main results are qualitatively similar therein.
- [107] Z. Cai and T. Barthel, Algebraic Versus Exponential Decoherence in Dissipative Many-Particle Systems, *Phys. Rev. Lett.* **111**, 150403 (2013).
- [108] Topological edge modes have been investigated recently in Refs. [109,110] in models without NHSE.
- [109] M. van Caspel, S. E. T. Arze, and I. P. Castillo, Dynamical signatures of topological order in the driven-dissipative Kitaev chain, *SciPost Phys.* **6**, 26 (2019).
- [110] M. J. Kastoryano and M. S. Rudner, Topological transport in the steady state of a quantum particle with dissipation, *Phys. Rev. B* **99**, 125118 (2019).
- [111] Y. Ashida and M. Ueda, Full-Counting Many-Particle Dynamics: Nonlocal and Chiral Propagation of Correlations, *Phys. Rev. Lett.* **120**, 185301 (2018).
- [112] B. Peng, Ş. K. Özdemir, F. Lei, F. Monifi, M. Gianfreda, G. L. Long, S. Fan, F. Nori, C. M. Bender, and L. Yang, Parity–time-symmetric whispering-gallery microcavities, *Nat. Phys.* **10**, 394 (2014).
- [113] V. V. Albert, Lindbladians with multiple steady states: Theory and applications, [arXiv:1802.00010](https://arxiv.org/abs/1802.00010).
- [114] L. Zhou, S. Choi, and M. D. Lukin, Symmetry-protected dissipative preparation of matrix product states, [arXiv:1706.01995](https://arxiv.org/abs/1706.01995).

Correction: A typographical error in the inline equation appearing after Eq. (14) has been fixed.